Macromolecules

pubs.acs.org/Macromolecules Article

Phase Behavior of Diblock Copolymer–Homopolymer Ternary Blends with a Compositionally Asymmetric Diblock Copolymer

Bo Zhang, Shuyi Xie, Timothy P. Lodge,* and Frank S. Bates*

Cite This: *Macromolecules* 2021, 54, 460–472 Read Online

ACCESS | Metrics & More | Article Recommendations | Supporting Information

ABSTRACT: The phase behavior of ternary polymer blends comprising poly(cyclohexylethylene) (C) and polyethylene (E) homopolymers and a compositionally asymmetric CE diblock copolymer with f_C = 0.67 was investigated, where f_C is the volume fraction of C. The morphology was established in the phase prism (volume fractions of C, E, and CE *vs* temperature) by optical transmission, small-angle X-ray scattering, and small-angle neutron scattering measurements. The locations of lamellar (LAM), hexagonally packed cylinders and gyroid ordered phases are shifted significantly toward lower fractions of the C homopolymer compared to previous results obtained from ternary polymer blends with a symmetric diblock copolymer (f_C = 0.5). Conversely, the Scott line of critical points, which delineates the boundary between single-phase disorder and macroscopic phase separation, remains virtually unchanged, coincident with the fraction of the C homopolymer associated with the binary homopolymer blend critical composition. A central finding of this study is that the line of nearly congruent order–disorder transitions, where the LAM phase melts virtually directly into the disordered state, is decoupled in composition from that of the Scott line of critical points. A wide range of phase space between the compositions associated with the congruent transition and Scott line was identified as containing a microemulsion morphology. This study demonstrates that diblock copolymer compositional asymmetry significantly impacts the ordered phase regime but has a marginal effect on the region displaying macroscopic phase separation. It also provides useful guidance for tuning the interfacial curvature, a crucial factor in the formation of bicontinuous microemulsions.

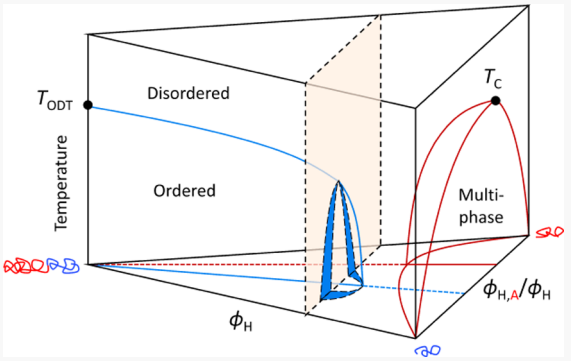

INTRODUCTION

Microemulsions, commonly encountered in ternary mixtures of water, oil, and surfactant, are thermodynamically stable disordered (DIS) structures with distinct microphase-separated water and oil domains, where the surfactant resides at the water/oil interface, preventing macroscopic phase separation.[1,2] A special type of microemulsion, the bicontinuous microemulsion (BμE), forms at specific temperatures and compositions, where the solubility of the surfactant becomes comparable in the water and oil phases, leading to interpenetrating co-continuous water and oil domains.[1−3] The temperature window where the BμE is observed, however, is relatively narrow due to complex intermolecular interactions between the water and surfactant. Ternary polymer blends of an AB diblock copolymer and the corresponding A and B homopolymers, which are high molecular weight analogues of water/oil/surfactant mixtures, show strikingly similar phase behavior. A BμE forms between the ordered lamellar phase (LAM) and multiphase coexistence regions in the vicinity of the order–disorder transition that separates the LAM and DIS states.[4−18] This polymeric BμE has been used as a template to create a host of functional materials, for example, for membrane applications.[19−25] Ternary polymer mixtures have unique advantages in designing bicontinuous structures due to the ability to precisely control component molecular weight, dispersity, and diblock copolymer composition. Moreover, in many systems, the intermolecular interactions are governed by simple van der Waals forces, and the overall phase behavior can be anticipated by mean-field theory. Thus, A/B/AB ternary polymer blends represent an ideal platform for exploring various states of order, macroscopic phase separation, and, most significantly, the intriguing microemulsion phase that exists at the boundary separating these limiting behaviors.

Phase behavior of ternary polymer mixtures is most effectively represented by a phase prism where the three corners at the base of the prism represent the pure components, and temperature forms the vertical axis. Three different "cuts" of the phase prism are commonly used to illustrate phase behavior: (i) an isothermal (constant temperature) plane; (ii) an isopleth (a plane with a constant ratio of

Received: July 27, 2020
Revised: November 4, 2020
Published: December 29, 2020

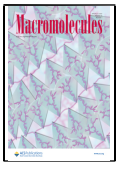

https://dx.doi.org/10.1021/acs.macromol.0c01745
Macromolecules 2021, 54, 460–472

homopolymer volume fractions and variable AB volume fractions); and (iii) a plane formed by a constant homopolymer (and AB) volume fraction. These three representations are shown in Figure 1. In this report, $\phi_{H,A}$ and ϕ_H refer to the volume fraction of homopolymer A and total homopolymer, respectively.

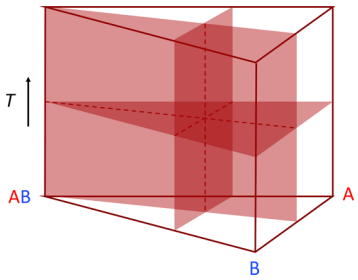

Figure 1. Schematic phase prism with three representative planes to describe the phase behavior of ternary polymer blends.

Depending on the composition and temperature, ternary mixtures of an AB diblock copolymer and the corresponding A and B homopolymers exhibit a variety of morphologies and phase transitions that fall into two universality classes: order−disorder phenomena, and critical behavior that separates a homogeneous DIS state and macroscopic phase separation. Volumetrically symmetric diblock copolymers form a LAM phase at high χN_{AB} and DIS at low χN_{AB}, where $\chi(T)$ is the Flory−Huggins interaction parameter and N_{AB} is the degree of polymerization of the diblock copolymer.[26−28] The LAM and DIS regions are separated by a second-order LAM−DIS transition at $\chi N_{AB} \approx 10.5$ in the context of mean-field theory.[29] Adding equal amounts of symmetric homopolymers swells the diblock copolymer, leading to an increase in the domain size.[30] Symmetric binary homopolymer blends, on the other hand, phase separate macroscopically at $\chi N \geq 2$, where $N_A = N_B = N$ is the volumetric degree of polymerization of the homopolymers.[27] Adding a symmetric diblock copolymer with $N_{AB} \approx 5N$ to the binary mixture increases the critical value $(\chi N)_c$ (*i.e.*, lowers the critical temperature when $\chi \sim T^{-1}$), creating a Scott line of critical points in the homopolymer-rich portion of the ternary phase space.[30] Within mean-field theory, the line of second-order LAM−DIS transitions and the Scott line of critical points meet at a Lifshitz point (LP), which is intersected by a three-phase window of LAM and two homopolymer-rich phases.[30,31] The LP appears at a total homopolymer volume fraction of $\phi_H = 1/(1 + 2\alpha^2)$ and $\chi N = 2(1 + 2\alpha^2)/\alpha$, where $\alpha = N/N_{AB}$.[30,31] At finite molecular weights, fluctuation effects impact each portion of the ternary phase space differently. The second-order ODT of diblock copolymers is replaced by a fluctuation-induced weakly first-order ODT,[32−37] consistent with the Brazovskii universality class.[38] Phase separation of binary homopolymer blends exhibits Ising-like critical behavior, instead of mean-field behavior, when close to the critical temperature.[39−42] As the diblock copolymer is added to the homopolymer mixture, a crossover occurs from Ising critical behavior to isotropic Lifshitz critical behavior as the composition moves along the Scott line of critical points, which terminates in the vicinity of the nominal LP.[43−48] The most dramatic effect induced by fluctuations is the formation of a region (previously referred to as a channel) of a thermodynamically stable BμE near the location of the mean-field-predicted LP. This intriguing state of nanoscale bicontinuity has been reported in ternary polymer blends with a variety of molecular weights and chemical structures[4−18] and in salt-doped and ionic ternary polymer blends.[49−53] These results, in concert with theoretical studies,[31,54,55] have led to the generally accepted conclusion that the LP is destroyed in any non-mean-field system due to fluctuation effects.

Recently, we identified the existence of a line of apparent congruent first-order LAM−DIS transitions in a symmetric ternary polymer blend, where the LAM phase transforms (virtually) directly to DIS, without passing through a two-phase coexistence of LAM and DIS.[12] (Recent theoretical calculations by Vorselaars *et al.* have established that what was identified as a condition of congruency by experiments is actually a very narrow region of coexistence between LAM and DIS phases with different ϕ_H.[56] This region spans $\Delta(\chi N) \approx 0.05$, which would be virtually indistinguishable from a congruent transition within experimental uncertainty. Hence, we continue to refer this as a congruent transition.) The congruent ODT was found to be coincident with the highest temperature associated with the envelope of LAM and 2-phase (LAM and DIS) states at each ϕ_H in the vicinity of the nominal LP composition $\phi_{H,LP}$. Curiously, the congruent ODT did not appear along the symmetric isopleth $\phi_{H,A} = 1/2$, even though the mixtures comprised a volumetrically symmetric diblock copolymer and symmetric homopolymers. Instead, the line of congruency appeared at approximately $\phi_{H,A}/\phi_H = 0.6$, coincident in composition with that of the A/B binary homopolymer blend critical point. Strikingly, the BμE channel along this congruent isopleth was reported to be unusually narrow (less than 1% in $\Delta\phi_H$). This finding raises the question of whether the asymmetry in the congruent ODT is in any way connected to the asymmetry of the binary blend critical point and the resulting Scott line.

To date, most research has focused on mixtures with symmetric diblock copolymers ($f_A = 0.5$) and homopolymers ($N_A = N_B$).[4−15] If the diblock copolymer is compositionally asymmetric, the ternary blend phase portrait, especially the copolymer-rich region, is expected to be skewed relative to the symmetric case, as the interfacial curvature is dominated by the presence of the diblock copolymer. In this work, we report the phase behavior of model saturated hydrocarbon polyolefin A/B/AB ternary mixtures, where A is poly(cyclohexylethylene) (C) and B is poly(ethylene) (E), with symmetric homopolymers and a compositionally asymmetric CE diblock copolymer ($f_C = 0.67$). In this case, the interfacial curvature is concave toward the minority block (E) of the diblock copolymer so that more E homopolymers are required to reverse the spontaneous curvature toward the E domains. This is indeed the case, as we find that the location of the ordered phases, along with the congruent ODT, is shifted significantly toward lower $\phi_{H,C}/\phi_H$, compared to the case where the diblock copolymer was compositionally symmetric.[12] Moreover, the congruent ODT is decoupled in composition (*e.g.* $\phi_{H,C}/\phi_H$) from the Scott line of critical points, which are coincident with the composition of the binary homopolymer blend critical point over the majority of the homopolymer-rich region. Between the disconnected endpoints of the congruent line and Scott line, a wide range of phase space is determined to contain a microemulsion morphology. Here, we present a schematic illustration (Figure 2) of the ternary phase prism that will be discussed in this report.

https://dx.doi.org/10.1021/acs.macromol.0c01745
Macromolecules 2021, 54, 460−472

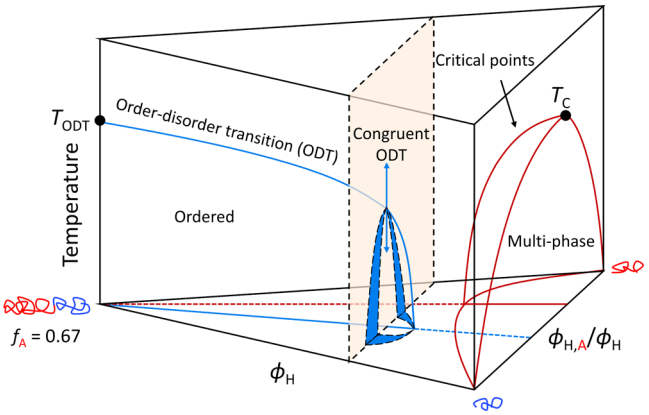

Figure 2. Schematic illustration of the phase behavior of ternary polymer blends with a compositionally asymmetric diblock copolymer and the corresponding symmetric homopolymers. Blue and red lines represent the phase boundary in ordered and multiphase regimes, respectively. The blue shaded envelope represents the coexistence between LAM and DIS.

EXPERIMENTAL SECTION

Polymer Synthesis, Characterization, and Blend Preparation. Poly(cyclohexylethylene) (C), poly(ethylene) (E), and poly(cyclohexylethylene)-*b*-poly(ethylene) (CE) were synthesized by catalytic saturation of polystyrene (S), 1,4-polybutadiene ($B_{1,4}$), and polystyrene-*b*-1,4-polybutadiene ($SB_{1,4}$), respectively, which were synthesized by anionic polymerization following established procedures.[57] Briefly, styrene and butadiene were purified rigorously over di-*n*-butylmagnesium and *n*-butyllithium, respectively, prior to use. Polymerizations of S, $B_{1,4}$, and $SB_{1,4}$ were performed in cyclohexane at 40 °C under a positive argon pressure, with *sec*-butyllithium as the initiator. The $SB_{1,4}$ diblock copolymer was synthesized by sequential polymerization of styrene and butadiene. The S homopolymer was catalytically deuterated using a Dow $PtRe/SiO_2$ catalyst in isooctane at 160 °C under 500 psi of D_2 for 12 h, leading to partially deuterium-labeled C. The $B_{1,4}$ homopolymer was hydrogenated using the same catalyst in cyclohexane at 110 °C for 12 h, resulting in E. The $SB_{1,4}$ diblock copolymer was hydrogenated in cyclohexane to generate CE. A typical hydrogenation reaction involved adding 10 g of polymer and 2 g of catalyst to 500 mL of solvent and reacting the solution with 500 psi of H_2 at 170 °C for 17 h.

The molecular weights and dispersities of the unsaturated homopolymers (S and $B_{1,4}$) were determined using a size exclusion chromatography (SEC) instrument equipped with a Waters 410 differential refractometer and calibrated with polystyrene standards, augmented with Mark−Houwink parameters. The molecular weight and dispersity of the unsaturated $SB_{1,4}$ diblock copolymer were determined using an SEC instrument equipped with a Wyatt Dawn Heleos II multiangle light scattering detector and a Wyatt Optilab rEX refractometer. The refractive index increment (dn/dc) was assumed to be the weight average of the dn/dc of each block (0.187 mL/g for S and 0.1295 mL/g for $B_{1,4}$). The C block volume fraction of the diblock copolymer was determined using proton nuclear magnetic resonance (^{1}H NMR) spectroscopy on the precursor $SB_{1,4}$ polymer and assuming melt densities reported at 140 °C (0.784 g/cm^3 for E and 0.92 g/cm^3 for C).[58] High-temperature SEC (Polymer Laboratories PL-GPC 220) measurements using 1,2,4-trichlorobenzene as the mobile phase at 135 °C were performed to confirm the chain integrity of each polymer after catalytic saturation. The number of deuterons per repeat unit of C was determined by comparing the ^{1}H NMR spectrum of the deuterated C with a hydrogenated C from the same S precursor, using 1,2,4-trichlorobenzene as an internal standard. The molecular weights of the saturated polymers were calculated based on the molecular weights of the precursor polymers, and the dispersities were obtained from the high-temperature SEC measurements. Characteristics of polymers are summarized in Table 1, and SEC traces are presented in the Supporting Information (Figure S1).

Table 1. Characteristics of Polymers

component	M_n (g/mol)	N^a	$Đ$	f_C
C[b]	2.5	38	1.09	
E	2.1	38	1.10	
CE[c]	18.2	293	1.18	0.67

[a]The volume degree of polymerization (N) was calculated based on a reference volume of 118 Å^3. [b]The C homopolymer used in optical transmission and SANS experiments has 6.2 deuterons per repeat unit, except that the C used for $\phi_{H,C}/\phi_H$ = 0.65 and ϕ_H = 0.8 has 5.4 deuterons per repeat unit. The C used in SAXS experiments was hydrogenated from the same precursor. [c]The CE diblock copolymer has an order−disorder transition temperature at 235 °C, determined using dynamic mechanical spectroscopy.

All samples discussed in this paper were prepared by co-dissolving appropriate amounts of each component in benzene at 70 °C. The solutions were then quickly immersed in liquid nitrogen, followed by freeze-drying under a dynamic vacuum for 24 h.

Optical Transmission Measurements. Optical transmission was measured using a home-built setup, comprising a 10 mW HeNe laser (633 nm) that passes through a neutral density filter to reduce the laser intensity, a lens to focus the transmitted light, and a photodiode detector to record the intensity. Samples were sealed in cylindrical ampoules under static vacuum and held in a large copper block with temperature control. Transmission was calculated based on the transmitted light intensity relative to a reference intensity and normalized to a scale of 0−100%. In a typical experiment, the sample was heated to a temperature above any phase transition and held until the transmitted intensity was stabilized. The sample was then cooled and heated at a rate of 1 °C/min. The transmitted light intensity was monitored over the entire cooling and heating transients.

Small-Angle X-ray Scattering. Small-angle X-ray scattering (SAXS) experiments were performed at the DND-CAT 5-ID-D beamline at the Advanced Photon Source of the Argonne National Laboratory, Argonne, Illinois, using a radiation wavelength λ = 0.7293 Å. Samples were loaded in differential scanning calorimetry (DSC) pans (DSC Consumables, Inc) and were heated to 200 °C for 30 min, slowly cooled to a desired temperature, and annealed for 24 h. Samples were then quickly immersed in liquid nitrogen after annealing to trap the blend morphology; the C and E materials used here have glass transition and melting temperatures of approximately 100 and 110 °C, respectively. At the beamline, samples were reheated directly to the desired temperature and annealed for 10 min before data collection. All 2D scattering patterns were cylindrically symmetric, and 1D plots of intensity *versus* scattering wave vector, $q = 4\pi \sin(\theta/2)/\lambda$, were obtained by azimuthally integrating the 2D scattering patterns, where θ is the scattering angle and q is the scattering vector.

Small-Angle Neutron Scattering. Small-angle neutron scattering (SANS) measurements were performed at the 30 m NG-7 beamline (University of Minnesota/Exxon Mobil/NIST) at the National Institute of Standards and Technology (NIST), Gaithersburg, Maryland, with a neutron wavelength of λ = 6 Å and a wavelength distribution of $\Delta\lambda/\lambda$ = 0.14, using three configurations (sample-to-detector distances of 13, 4, and 1 m). Samples were loaded either into home-built quartz banjo cells with a nominal thickness of 1 mm or sandwiched between two quartz windows with an aluminum spacer (0.8 mm thick). The exact thickness of each home-built banjo cell was determined by measuring the overall cell thickness and subtracting the known quartz window thickness, while the aluminum spacers were measured with a caliper. Samples for critical scattering measurements were loaded into banjo cells and heated to at least 20 °C above the phase separation temperature determined by transmission measurements. Then, the cells were quickly immersed in a liquid nitrogen bath to fix the one-phase morphology. At the

https://dx.doi.org/10.1021/acs.macromol.0c01745
Macromolecules 2021, 54, 460−472

beamline, these samples were heated directly to a temperature at least 20 °C above the phase separation temperature and then cooled to a series of measurement temperatures, with at least 10 min of annealing at each temperature prior to data collection. Microemulsion samples were heated to 220 °C, slowly cooled to desired temperatures, and annealed for at least 15 min before data collection. All scattering patterns were azimuthally symmetric and reduced to 1D profiles using software developed by the NIST Center for Neutron Research for Igor Pro. Scattering data were corrected for sample thickness, transmission, background, and empty cell scattering and calibrated to an absolute intensity scale by direct measurement of the neutron flux. Incoherent scattering was estimated based on the volume fraction average of the high q scattering intensity measured for each pure homopolymer and was subtracted from the total blend scattering intensity prior to model fitting.

RESULTS

Ordered Phase Morphologies. The ordered phase morphologies in the copolymer-rich portion of the phase prism were determined using SAXS experiments. Representative SAXS patterns obtained at 140 °C for samples at $\phi_H = 0.1$, $\phi_H = 0.3$, $\phi_H = 0.65$, and $\phi_H = 0.8$ with different $\phi_{H,C}/\phi_H$ are presented in Figure 3a–d, respectively. At $\phi_H = 0.1$, two distinct patterns, consistent with gyroid (GYR) and hexagonally packed cylinders (HEX) phases, are evident. The GYR phase at $\phi_{H,C}/\phi_H = 0$ is associated with Bragg peaks at $q/q^* = \sqrt{6}, \sqrt{8}, \sqrt{14}$, and $\sqrt{16}$, while the HEX phase assigned at $\phi_{H,C}/\phi_H = 0.5$ and 1 is based on Bragg peaks at $q/q^* = \sqrt{1}, \sqrt{3}, \sqrt{4}, \sqrt{7}$, and $\sqrt{9}$, where q^* is the first scattering peak. Calculations indicate that the missing peak at $q/q^* = \sqrt{3}$ for HEX can be attributed to form factor extinction (Figure S2). Increasing the homopolymer content to $\phi_H = 0.3$ leads to Bragg peaks at $q/q^* = \sqrt{1}, \sqrt{4}$, and $\sqrt{9}$, which can be associated with a LAM phase. Increasing $\phi_{H,C}/\phi_H$ to 0.5 leads to GYR, while HEX is observed at $\phi_{H,C}/\phi_H = 0.6$. At $\phi_H = 0.65$ and 0.8, the only ordered morphology identified is LAM. Note that for samples with $\phi_H \geq 0.8$, the scattering peaks broaden and higher-order peaks become difficult to identify due to the swollen and less coherent state of the lamellae at these compositions. When the ratios of C/E fractions are highly asymmetric (*e.g.*, $\phi_{H,C}/\phi_H$ close to 1), the mixtures show scattering behavior which we associate with differently structured DIS states. We point out that no phase boundaries exist among these DIS phases, which include fluctuating DIS states in the copolymer-rich region, homogeneous single phases in the homopolymer-rich region, and microemulsions between these two limiting cases. A representative scattering pattern, consistent with a microemulsion state, from the specimen at $\phi_{H,C}/\phi_H = 0.8$ and $\phi_H = 0.6$ is shown in Figure 3d. Detailed analysis of microemulsion structures interrogated by SANS will be discussed below. Figure 4 shows a compendium of the ordered state phase assignments deduced from the SAXS measurements obtained at 140 °C. This isothermal ternary phase diagram also identifies the locations of the multiphase and microemulsion states based on the cloud point and SANS measurements as described below.

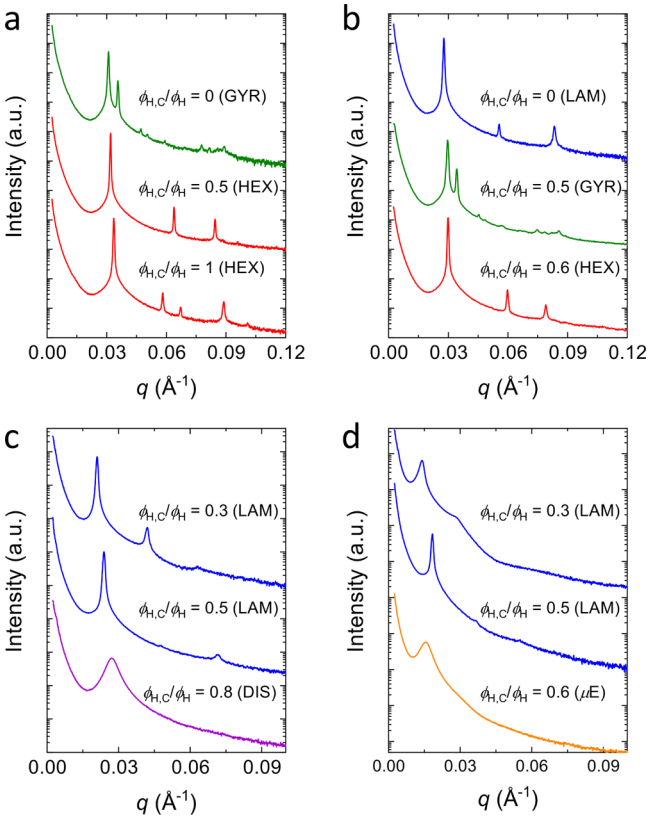

Figure 3. Representative SAXS patterns obtained at 140 °C across planes with a constant homopolymer content but varying homopolymer composition: (a) $\phi_H = 0.1$, (b) $\phi_H = 0.3$, (c) $\phi_H = 0.65$, and (d) $\phi_H = 0.8$ with different $\phi_{H,C}/\phi_H$.

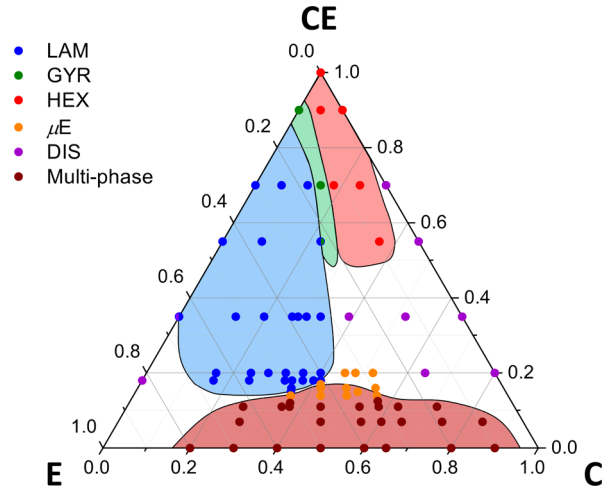

Figure 4. Isothermal phase diagram at 140 °C is presented, with each corner as the pure component. All lines are drawn to guide the eye. Phase coexistence required in ternary mixtures between each one-phase region is not shown for simplicity.

Congruent Transition. Optical transmission was recently identified as an efficient method for detecting phase coexistence between the LAM and DIS states in C/E/CE ternary blends.[12] Because the coexisting LAM and DIS phases in a two-phase region have different compositions, they have slightly different refractive indices. This results in light scattering and therefore a reduction in optical transmission. Conversely, at the point of congruency, birefringent LAM grains melt directly into the isotropic DIS phase, leading to a step increase in optical transmission, without evidence of light scattering.[59] We have used the same technique to locate the congruent ODT in this study. Representative optical transmission data obtained while heating and cooling several specimens are shown in Figure 5. Figure 5a illustrates the

https://dx.doi.org/10.1021/acs.macromol.0c01745
Macromolecules 2021, 54, 460−472

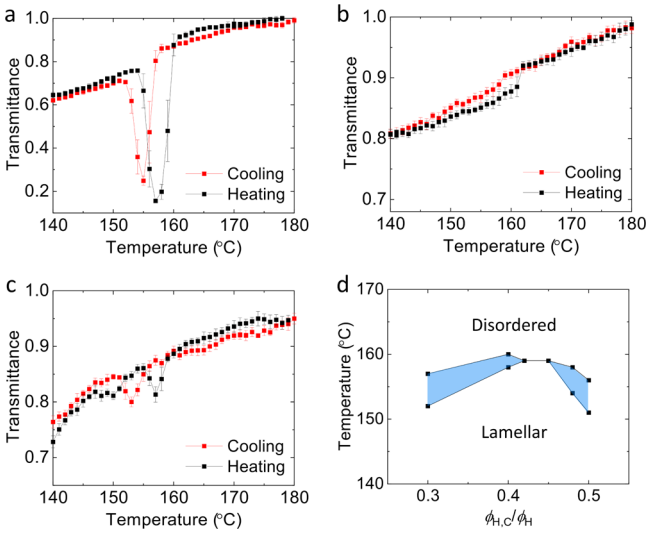

Figure 5. Selected optical transmission measurements for samples within the plane at ϕ_H = 0.82 with various ratios of C/E homopolymer fractions: (a) $\phi_{H,C}/\phi_H$ = 0.3, (b) $\phi_{H,C}/\phi_H$ = 0.42, and (c) $\phi_{H,C}/\phi_H$ = 0.5 with a cooling and heating rate of 1 °C/min. (d) Phase diagram for the plane at ϕ_H = 0.82 with the blue region as the coexistence between LAM and DIS.

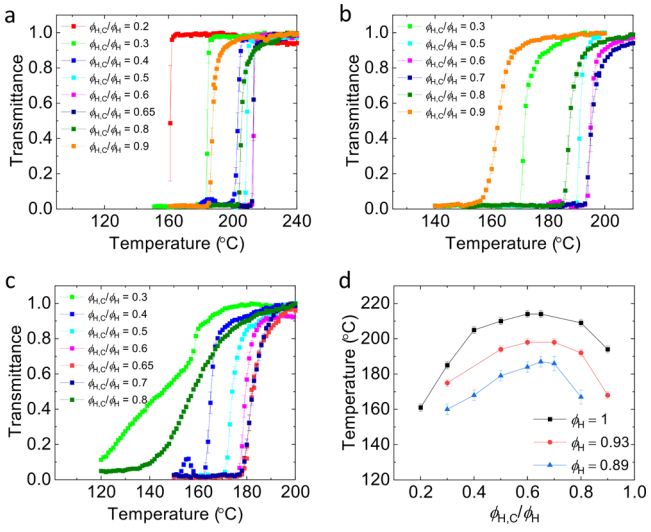

Figure 6. Cloud point measurements for samples with a homopolymer content of (a) ϕ_H = 1, (b) ϕ_H = 0.93, and (c) ϕ_H = 0.89 with various $\phi_{H,C}/\phi_H$. The data were collected during cooling ramps. (d) Summary of cloud points at planes with different ϕ_H.

transmission results recorded for ϕ_H = 0.82 and $\phi_{H,C}/\phi_H$ = 0.3, which reveals a pronounced dip in the optical signal between approximately 150 and 160 °C upon cooling and heating at 1 °C/min. This result, including the slight hysteresis, is consistent with traversing a LAM−DIS 2-phase coexistence region, similar to the phenomena reported earlier.[12] It also demonstrates the reversibility of the phase transition between ordered and DIS structures. The range of the "optical dip" during cooling was used to establish the phase coexistence boundaries of the LAM and DIS phases. The optical transmission for ϕ_H = 0.82 and $\phi_{H,C}/\phi_H$ = 0.42, shown in Figure 5b, shows a distinctly different pattern from Figure 5a. A step increase in optical transmission upon heating, and step decrease upon cooling, occurs at approximately 160 °C. We associate this behavior with a state of congruency. Note that the congruent transition occurs approximately at the highest T_{ODT}, consistent with the previous report.[12] Adjusting the composition to ϕ_H = 0.82 and $\phi_{H,C}/\phi_H$ = 0.5 leads to another "optical dip", with hysteresis, between 152 and 160 °C (Figure 5c). The phase behavior for the plane with ϕ_H = 0.82 in the phase prism, determined from the optical transmission and SAXS measurements, is presented in Figure 5d, with the blue shaded area denoting the LAM−DIS coexistence region. Similar phase behavior was observed at ϕ_H = 0.65, as presented in Figure S3.

Cloud Points. The boundary between one-phase and multiphase regions in the limit of low diblock copolymer content, denoted as binodal points, was determined by measuring the optical transmission while cooling at 1 °C/min from the one-phase state. The binary homopolymer mixtures (ϕ_H = 1) first turn cloudy upon cooling into the two-phase region and then separate into two clear layers, usually within 20 min. Conversely, samples at ϕ_H = 0.93 and 0.89 remain cloudy during the entire measurement period of approximately 2 h when the specimens are in the two-phase region. Cloud point results for mixtures at ϕ_H = 1, 0.93, and 0.89 with various $\phi_{H,C}/\phi_H$ are shown in Figure 6a−c, respectively. We estimate the binodal condition as the point where the transmission has dropped to 85% of the maximum value. A summary of the cloud points determined at each composition is plotted in Figure 6d. Interestingly, even though the C and E homopolymers are symmetric in volume, the phase boundary for the binary mixture is not symmetric. We estimate the critical point of the binary C/E blend by fitting the cloud point data with the Flory−Huggins theory (Figure S4), with a composition-dependent χ (*e.g.*, $\chi = (\alpha/T + \beta)(1 + c\phi_{H,C})$), where α, β, and c are fitting parameters.[60,61] (We point out that fluctuation effects are ignored when using the Flory−Huggins theory, a mean-field approach to model the binary blend phase behavior). The critical composition is approximately at $\phi_{H,C}/\phi_H$ = 0.65, where the peak cloud point temperature appears. Similarly, for mixtures at ϕ_H = 0.93 and 0.89, the peak temperature occurs at approximately $\phi_{H,C}/\phi_H$ = 0.65. The cloud point measurements suggest that the Scott line of critical points follows the binary polymer blend critical point composition, assuming that the cloud point data follow the Flory−Huggins theory. We note that although the Flory−Huggins theory describes the phase behavior of binary polymer blends quite well, there is no requirement for a critical point to appear at the highest cloud point temperature, especially when ϕ_H is close to the Lifshitz composition $\phi_{H,LP}$. Nevertheless, SANS measurements, discussed below, show that the blends associated with the highest cloud point temperatures for ϕ_H = 1 and 0.93 exhibit critical scattering within several degrees of the phase transition, while the composition at the peak temperature for ϕ_H = 0.89 is slightly off-critical.

Critical Scattering. Specimens at $\phi_{H,C}/\phi_H$ = 0.65 and ϕ_H = 1, 0.93, and 0.89 were investigated as a function of temperature above the cloud point temperature by SANS. In general, scattering from isotropic homogeneous multicomponent mixtures derives from concentration fluctuations. At a stability limit (*i.e.*, spinodal point), the concentration fluctuations diverge in the length scale, resulting in divergence in scattered intensity at q = 0.[62] The only point in the phase space where such behavior can be accessed is the critical point, where the binodal and spinodal curves are coincident. Off-critical mixtures will phase separate before reaching the spinodal point, eliminating critical scattering. Critical phenom-

https://dx.doi.org/10.1021/acs.macromol.0c01745
Macromolecules 2021, 54, 460−472

ena along the Scott line of critical points have been investigated by several groups. At $\phi_H = 1$, inverse scattering patterns ($I^{-1}(q)$) are linear in q^2 and follow the Ising critical behavior at temperatures close to the critical temperature.[39−42] Adding a diblock copolymer to such mixtures requires inclusion of both q^2 and q^4 terms simultaneously to describe the scattering patterns.[43−48] At ϕ_H close to $\phi_{H,LP}$, inverse scattering patterns become linear in q^4, indicative of the Lifshitz critical behavior.[43−48]

SANS patterns (I *vs* q) for $\phi_{H,C}/\phi_H = 0.65$ with $\phi_H = 1$ and 0.93 obtained at various temperatures are presented in Figure 7a,b. Figure 7c,d shows these data plotted in the Ornstein−

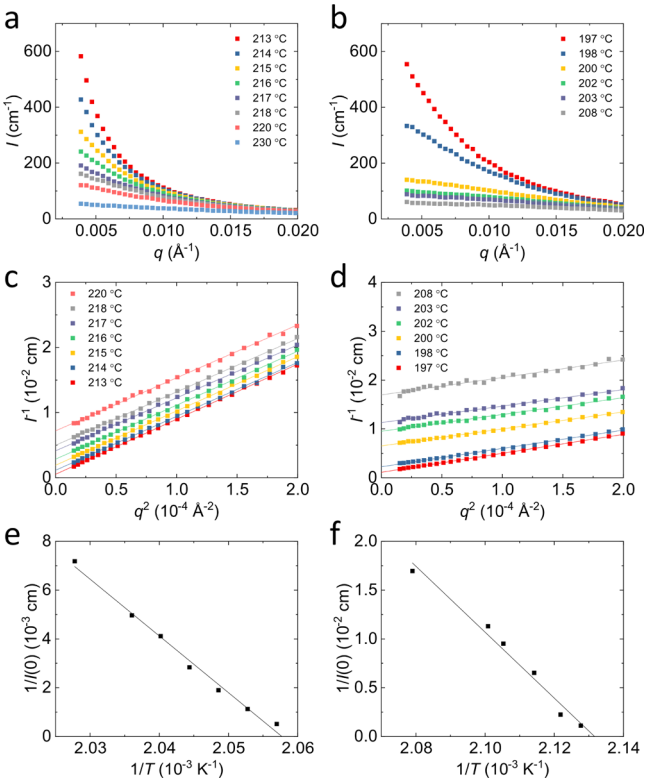

Figure 7. (a,b) SANS patterns (I *vs* q), (c,d) I^{-1} *vs* q^2, and (e,f) $I^{-1}(0)$ *vs* $1/T$ for samples at $\phi_H = 1$ and 0.93, with $\phi_{H,C}/\phi_H = 0.65$, respectively.

Zernike form, $I^{-1}(q)$ *versus* q^2. Both sets of results produce linear correlations that have been extrapolated to $q = 0$. Figures 7e,f present $I^{-1}(0)$ *versus* $1/T$, again generating linear correlations, which have been extrapolated to $I^{-1}(0) = 0$, yielding the temperatures associated with the stability limit for these mixtures. The fact that in both cases the extrapolated temperature is within 1 °C of the lowest measurement temperature indicates that $\phi_{H,C}/\phi_H = 0.65$ corresponds to the composition of the Scott line.

Adding more diblock copolymers to the homopolymer mixture changes the SANS results, as shown in Figure 8 for $\phi_{H,C}/\phi_H = 0.65$ and $\phi_H = 0.89$. A comparison of Figure 8a with Figure 7a,b reveals that the former mixture is less responsive to changes in temperature than the mixtures with less diblock copolymers. Increasing the copolymer concentration requires us to add a q^4 term to model the scattering patterns. In fact, the data become linear in q^4 instead of q^2, as demonstrated in Figure 8b, consistent with the Lifshitz critical behavior. Extrapolation to $q = 0$ yields $I^{-1}(0)$, which is plotted *versus*

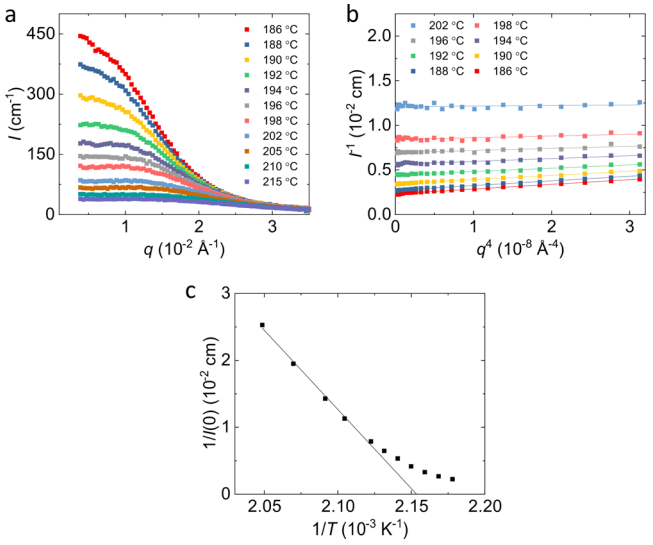

Figure 8. (a) SANS patterns, (b) I^{-1} *vs* q^2, and (c) $I^{-1}(0)$ *vs* $1/T$ for the sample at $\phi_{H,C}/\phi_H = 0.65$ and $\phi_H = 0.89$.

$1/T$ in Figure 9c. In this case, in contrast to Figure 7e,f, the result deviates significantly from linearity, which has been

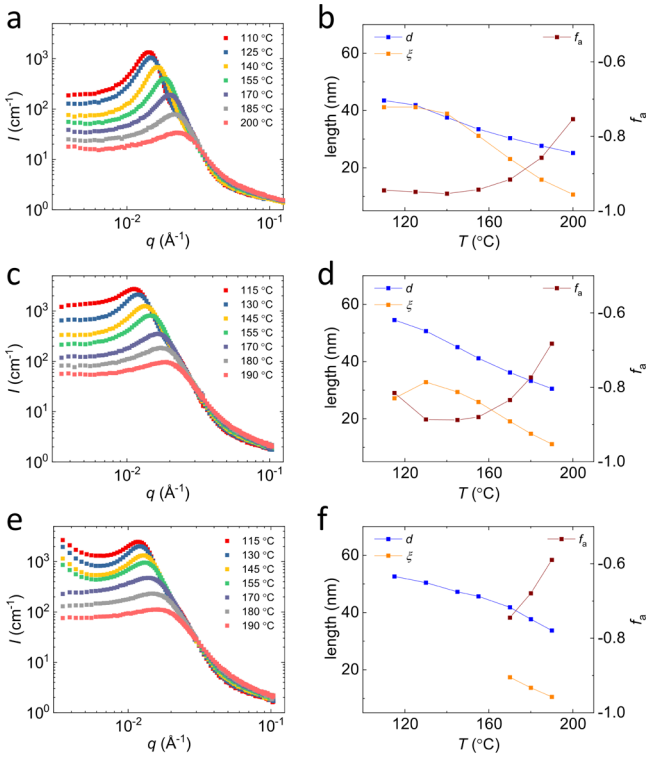

Figure 9. SANS patterns (left) and extracted structure information (right) at various temperatures by fitting with the Teubner−Strey (T−S) model for samples along the isopleth of $\phi_{H,C}/\phi_H = 0.65$ and (a,b) $\phi_H = 0.8$, (c,d) $\phi_H = 0.84$ and (e,f) $\phi_H = 0.86$.

attributed to fluctuation effects.[44−48] This sample seems to be slightly off-critical as $I^{-1}(0)$ at the lowest measurement temperature before phase separation is not as close to 0 as the samples at $\phi_H = 1$ and 0.93. We have investigated two additional samples with $\phi_H = 0.89$ and $\phi_{H,C}/\phi_H = 0.6$ and 0.7 (Figure S5). The sample at $\phi_{H,C}/\phi_H = 0.6$ shows very similar scattering behavior to the mixture at $\phi_{H,C}/\phi_H = 0.65$, while the

https://dx.doi.org/10.1021/acs.macromol.0c01745
Macromolecules 2021, 54, 460−472

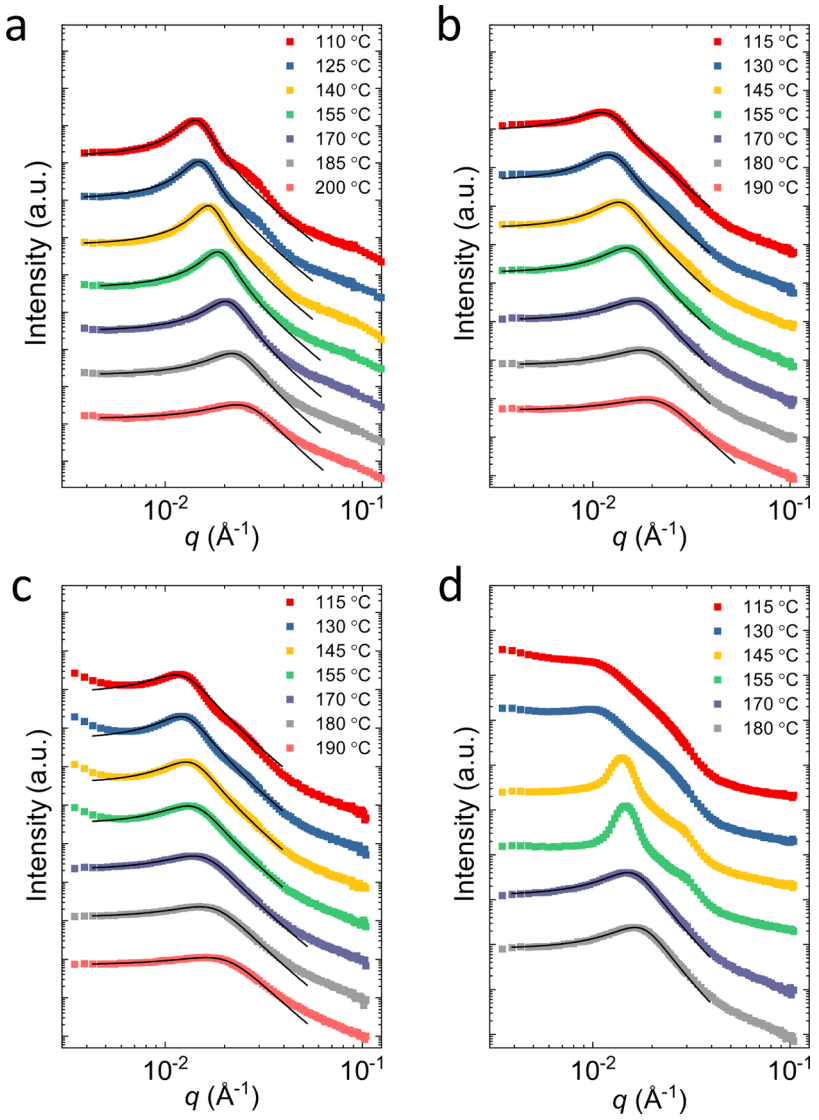

Figure 10. SANS patterns fitted with the T−S model (black lines) for samples at $\phi_{H,C}/\phi_H = 0.65$ with (a) $\phi_H = 0.8$, (b) $\phi_H = 0.84$, and (c) $\phi_H = 0.86$. (d) SANS patterns for $\phi_{H,C}/\phi_H = 0.42$ and $\phi_H = 0.84$. Data at 170 and 180 °C were fitted with the T−S model. Data have been vertically shifted for clarity.

sample at $\phi_{H,C}/\phi_H = 0.7$ is clearly further off-critical. We believe that this places the critical composition between $\phi_{H,C}/\phi_H = 0.6$ and 0.65. Therefore, we conclude that the Scott line of critical points follows the binary blend critical composition over the majority of the homopolymer-rich portion of the phase prism and curves slightly toward the center of the phase prism as the homopolymer composition decreases from $\phi_H = 0.93$ to 0.89.

Microemulsions. BμEs have been reported in numerous systems that locate between the ordered LAM and multiphase regions with a width in $\Delta\phi_H$ between 1 and 4%. In this study, the microemulsion channel along the congruent isopleth is indeed very narrow at certain temperatures, similar to our previous report dealing with C/E/CE ternary blends.[12] The region in the phase space where microemulsions appear gradually broadens (in terms of $\Delta\phi_H$) when moving from the congruent composition to the Scott line composition. Representative specimens were studied by SANS experiments as a function of temperature. We present selected SANS patterns for samples along the Scott line composition in Figure 9. In general, scattering patterns from microemulsions show a single broad peak at finite q with a characteristic q^{-4} decay at high q. Figures 9a,c,e present the SANS patterns from samples at $\phi_{H,C}/\phi_H = 0.65$, with $\phi_H = 0.8$, 0.84, and 0.86. Overall, the mixture at $\phi_H = 0.8$ and $\phi_{H,C}/\phi_H = 0.65$ exhibits scattering patterns consistent with well-structured microemulsions over the entire measured temperature range. Increasing the homopolymer concentration to $\phi_H = 0.84$ and $\phi_{H,C}/\phi_H = 0.65$ results in a slightly different result, where the principal scattering peak at 115 °C appears broader than that at 130 °C. We associate this feature with phase separation, which becomes more apparent in the mixture at $\phi_H = 0.86$ and $\phi_{H,C}/\phi_H = 0.65$ at and below 155 °C. As demonstrated in Figure 9e, the scattering patterns show a single broad peak with a characteristic q^{-4} decay at temperatures greater than 155 °C. At lower temperatures, however, a distinctive upturn at low q is observed, indicative of the existence of large-scale structures. Moreover, the sample turns turbid at these temperatures. Thus, we conclude that the mixture transforms from a single-phase microemulsion into multiple phases.

https://dx.doi.org/10.1021/acs.macromol.0c01745
Macromolecules 2021, 54, 460−472

Additionally, the main peak that is associated with the microemulsion phase persists at temperatures lower than 155 °C, which implies that it is a microemulsion phase that coexists with one or two homopolymer-rich phases. In fact, phase coexistence is seen over a wide range of the phase space as shown in Figure 4. A similar phenomenon, that is, a microemulsion channel cut off by a multiphase region, has been observed previously in a similar ternary polymer blend.[7] In general, the appearance of such phase coexistence is due to the increase in segregation strength between each component as the temperature is reduced and/or the homopolymer concentration is increased, until the point where the diblock copolymer cannot accommodate any more homopolymer. Beyond this point, excess homopolymer is swept out from the microemulsion domain, forming one or two homopolymer-rich phases.

Structural information associated with the microemulsions was extracted by fitting the scattering profiles to the Teubner-Strey (T−S) model (eq 1), which was originally developed to describe the scattering from microemulsions of water/oil/surfactant mixtures.[63] Three parameters were extracted: domain spacing (d), correlation length (ξ), and amphiphilicity factor (f_a), as defined in eqs 2−4, respectively.[63,64] The domain spacing describes the periodicity of the nanostructure; the correlation length describes how far the structural correlation persists; and the amphiphilicity factor describes how well the interfacial agent, diblock copolymer in this case, stabilizes the microemulsion. A LAM structure has $f_a = -1$, and a "good" microemulsion has $-1 < f_a < 0$.

$$I(q) = \frac{1}{a_2 + c_1 q^2 + c_2 q^4} \tag{1}$$

$$d = 2\pi \left[\frac{1}{2}\left(\frac{a_2}{c_2}\right)^{1/2} - \frac{1}{4}\left(\frac{c_1}{c_2}\right) \right]^{-1/2} \tag{2}$$

$$\xi = \left[\frac{1}{2}\left(\frac{a_2}{c_2}\right)^{1/2} + \frac{1}{4}\left(\frac{c_1}{c_2}\right) \right]^{-1/2} \tag{3}$$

$$f_a = \frac{c_1}{\sqrt{4 a_2 c_2}} \tag{4}$$

The T−S fitting is presented in Figure 10, and the extracted structural information is summarized in Figures 9b,d,f for the mixtures at $\phi_H = 0.80$, $\phi_H = 0.84$, and $\phi_H = 0.86$ with $\phi_{H,C}/\phi_H = 0.65$, respectively. All three samples are well-structured microemulsions as the amphiphilicity factor is smaller than 0. Note that the specimen at $\phi_H = 0.86$ is complicated by phase separation at low temperatures. Therefore, the correlation length and amphiphilicity factor (not shown) cannot be extracted due to the low q upturn. Overall, the domain spacing and correlation length for each sample decrease upon heating, suggesting increased interfacial mixing and interpenetrating of each component. This is consistent with the increase in the amphiphilicity factor, indicating that the microemulsion becomes less structured. The domain spacing of the sample at $\phi_H = 0.8$ is much smaller than the ones at $\phi_H = 0.84$ and 0.86 at equivalent temperatures. This is due to a higher amount of homopolymer that further swells the microemulsion domains. We also present the SANS results for the specimen along the congruent isopleth at $\phi_H = 0.84$ and $\phi_{H,C}/\phi_H = 0.42$ in Figure 10d. At temperatures between 170 and 180 °C, this sample exhibits scattering behavior consistent with microemulsions. The data were fitted with the T−S model, and the domain spacing, correlation length, and amphiphilicity factor are 39.9, 20.8 nm, and −0.83 for 170 °C and 36.5, 18.2 nm, and −0.82 for 180 °C, which are approximately the same with those of the mixture at $\phi_H = 0.84$ and $\phi_{H,C}/\phi_H = 0.65$. At lower temperatures, these two samples exhibit different behaviors. The mixture along the congruent isopleth forms LAM (indicated by the Bragg peaks at $q/q^* = 1, 2$), while the one along the Scott line composition develops better structured microemulsions but remains DIS. Phase separation, indicated by the low q upturn of the congruent mixture at $\phi_H = 0.84$, occurs below 145 °C. For certain samples (*e.g.*, $\phi_H = 0.8$ and 0.84 with $\phi_{H,C}/\phi_H = 0.65$), a secondary shoulder at approximately $q/q^* = 2$ was observed at temperatures below 150 °C (see Figure 10a−c), which is not captured by the T−S model. This feature, recorded previously in a light scattering study of spinodal decomposition in a binary polymer blend,[65] and in SANS measurements of DIS symmetric block copolymers near T_{ODT},[35] has been attributed to strongly segregated domains.

DISCUSSION

We have demonstrated the phase behavior of ternary blends composed of a compositionally asymmetric CE diblock copolymer ($f_C = 0.67$) and a pair of compositionally symmetric C and E homopolymers. Although A/B/AB ternary blends have been studied for the past 20 years, to the best of our knowledge, this is the first report of the effects of the diblock copolymer compositional asymmetry on ternary blend phase behavior and the first study that experimentally characterizes the phase boundary across the entire phase prism. In this section, we first compare the current study to a previous investigation of a similar C/E/CE blend but with a symmetric diblock copolymer[12] and then discuss the main findings and implications from this investigation.

Relation to Prior Studies. Most investigations related to A/B/AB ternary blends in the past two decades have focused on the volumetrically symmetric isopleth of the phase prism. These studies have established the ODT in the copolymer-rich region ($0 < \phi_H < \phi_{H,LP}$), critical phenomena in the homopolymer-rich region ($\phi_{H,LP} < \phi_H < 1$), and a channel of BμE that appears in the vicinity of the predicted LP between these two limiting cases. Recently, we have mapped the phase behavior of the ordered region for a similar but compositionally symmetric ($f_C = 0.5$, $N_C \approx N_E \approx 0.2N_{CE}$) C/E/CE ternary polymer blend.[12] One of the key findings was a line of congruent LAM−DIS transitions at approximately $\phi_{H,C}/\phi_H = 0.6$. This congruent transition occurred at the peak temperature of the envelope of LAM and LAM−DIS 2-phase coexistence for each plane of compositions ϕ_H near the Lifshitz composition $\phi_{H,LP}$. The principal source of asymmetry that causes the appearance of the congruent melting at $\phi_{H,C}/\phi_H = 0.6$ instead of at $\phi_{H,C}/\phi_H = 0.5$ for the symmetric ternary mixture was identified as the conformational asymmetry. Note that the conformational asymmetry is different from compositional asymmetry, which is the focus of this report. Conformational asymmetry, $\varepsilon = (b_A/b_B)^2$, captures the difference in the statistical segmental length (b) of each block. It has been shown to have significant influence on the phase behavior of diblock copolymers,[66−69] binary homopolymer blends,[70] and ternary polymer blends discussed here.[7,12,71] In the present

https://dx.doi.org/10.1021/acs.macromol.0c01745
Macromolecules 2021, 54, 460−472

case, C and E have segmental lengths of 4.6 and 8.3 Å, respectively, based on a reference volume of 118 Å^3, resulting in virtually the largest conformational asymmetry, ε = 3.3, among pairs of common flexible polymers.[58] Therefore, even though each block occupies essentially the same molecular volume in a compositionally symmetric diblock copolymer (f_C = 0.5), they pervade space quite differently due to the difference in b. The block with a larger b, E in this case, has a larger radius of gyration, while having the same occupied volume as the C block. This asymmetry in the pervaded volume of each block of the CE diblock copolymer gives rise to a difference in the entropic penalty of stretching: a block with a larger radius of gyration has a lower entropic cost of stretching.[66,67] At a curved interface in incompressible liquids, the inner domain has to stretch more to maintain the same density. Therefore, in the limit of pure CE diblock copolymers, interfaces prefer to curve toward the E domain to reduce the entropic cost of stretching. Hence, the overall phase diagram is shifted toward higher f_E.[66,67] Adding low molecular weight diluents, however, can reverse the preferred interfacial curvature. As the E block has a larger radius of gyration, it can be swelled more easily by low molecular weight homopolymers (*e.g.*, in the wet brush limit) than the C block, shifting the spontaneous curvature toward the C block with addition of equal amounts of each homopolymer (*i.e.*, along the volumetrically symmetric isopleth, $\phi_{H,C}/\phi_H$ = 0.5). This spontaneous curvature can be compensated for by adding more C homopolymers, leading to the appearance of the congruent transition at $\phi_{H,C}/\phi_H > 0.5$ when the mixtures are in the swollen state (*e.g.*, ϕ_H close to $\phi_{H,LP}$). This is the argument advanced by Hickey *et al.* to explain the phase behavior of the compositionally symmetric C/E/CE system.[12]

Notably, the composition of the congruent line in the symmetric ternary system is nearly coincident with the homopolymer blend critical point ($\phi_{H,C}/\phi_H$ = 0.63).[12] The BμE channel, bracketed by a line of congruent first-order LAM−DIS transitions and a Scott line of critical points, spans a channel less than 1% wide in $\Delta\phi_H$. This result spawned the hypothesis that the line of congruent transitions and Scott line of critical points are coupled in the composition space in the phase prism. Although this seems to occur for symmetric mixtures, there is no reason to expect the congruent composition to track the Scott line composition in general, for example, if we break the diblock copolymer symmetry.

Decoupled Congruency and Criticality. Because the interfacial curvature is strongly influenced by the presence of diblock copolymers, we expect the ternary blend phase behavior to be skewed relative to the symmetric case, especially in the copolymer-rich region due to the compositionally asymmetric CE diblock copolymer. Two factors favor interfacial curvature that is concave toward the E block of the diblock copolymer: the asymmetric composition with a lower volume fraction of E and the larger statistical segment length for E *versus* C as described in the previous section. Hence, more E homopolymers are required to reverse the spontaneous curvature toward the E domains. This is indeed the case, as seen in Figure 4. At $\phi_H < 0.3$, only GYR and HEX morphologies with C as the matrix are found. LAM first appears at ϕ_H = 0.3 and is restricted to $\phi_{H,C}/\phi_H < 0.5$ as the homopolymer content increases. Moreover, we have not observed any morphologies with a continuous matrix of E. This asymmetric phase behavior was further demonstrated by optical transmission measurements, which established the congruent LAM−DIS transition at $\phi_{H,C}/\phi_H$ = 0.42. Recall that the congruent ODT appeared at $\phi_{H,C}/\phi_H$ = 0.6 for the compositionally symmetric C/E/CE ternary blend.[12] Here, compositional asymmetry overwhelms the effects of conformational asymmetry, shifting the entire ordered state phase portrait, along with the line of congruent transitions, to the low $\phi_{H,C}/\phi_H$ side of the phase prism (Figure 4). This result offers the opportunity to ascertain the relationship between the condition of congruency, which we associate with the zero mean curvature above and below the ODT, and the position of the Scott line in the vicinity of the Lifshitz composition in the phase prism.

A crossover from Ising critical behavior to isotropic Lifshitz behavior along the Scott line of critical points, along with the extinction of the LP in the finite molecular weight (non-mean-field) mixtures, has been well established.[31,43−48,54,55] In this study, we have mapped the phase boundary in the multiphase region with a focus on identifying the location of the Scott line. The key finding is a line of critical points that primarily follows the location of the binary homopolymer blend critical point and which is decoupled in composition from the line of congruent transitions. At $\phi_H \geq 0.93$, the Scott line of critical points is coincident with the location of the binary blend critical point ($\phi_{H,C}/\phi_H$ = 0.65). This trend deviates only slightly in the Lifshitz regime ($I^{-1}(q)$ linear with q^4), with the critical composition estimated to fall between $\phi_{H,C}/\phi_H$ = 0.6 and 0.65 at ϕ_H = 0.89. These two samples ($\phi_{H,C}/\phi_H$ = 0.6 and 0.65) show very similar scattering patterns (Figures 8a and S5a), which suggests that the actual critical point lies at a composition between these two limits (*e.g.*, $\phi_{H,C}/\phi_H \approx 0.62$).

Apparently, the diblock copolymer compositional asymmetry exerts a much less significant influence on the phase behavior of the multiphase region *versus* the ordered phase region, which exhibits a decidedly asymmetric phase portrait (Figure 4). The congruent composition represents a state of delicately balanced interfacial tension and curvature, while no interface exists in the single-phase critical mixtures. Accordingly, breaking the diblock copolymer symmetry will unavoidably shift the ordered phase portrait but should have less influence on the critical mixtures, as found here. Thus, the apparent coupling between the congruent line and Scott line reported earlier is a coincidence due to the compositionally symmetric CE diblock copolymer.

The composition dependence of the Scott line can be estimated using the mean-field Flory−Huggins model, applied to the three components, as described in the Supporting Information. Figure S6 presents the result of calculations dealing with a ternary blend of symmetric homopolymers and a compositionally asymmetric diblock copolymer (f_A = 0.55, $N_A = N_B = 0.2N_{AB}$); here, we have assumed conformational symmetry. These calculations indicate that a compositionally asymmetric diblock copolymer rich in A leads to curved envelopes of instability and the associated critical points that increasingly bend toward lower $\phi_{H,A}/\phi_H$ with increasing χN. These calculations anticipate significantly greater shifts in the location of the Scott line with the diblock copolymer compositional asymmetry than what we observe experimentally, where the line of critical points remains nearly constant in composition ($\phi_{H,C}/\phi_H \approx 0.65$) between ϕ_H = 0.89 and 1. This may be a consequence of the relatively low molecular weight polymers used in the experiments, which amplifies fluctuation effects. Here, we note that the binary blend (ϕ_H = 1) critical point does not appear at the symmetric condition $\phi_{H,C}/\phi_H$ =

https://dx.doi.org/10.1021/acs.macromol.0c01745
Macromolecules 2021, 54, 460−472

0.5, even though the molecular volumes of the two components are nearly equal. We attribute this behavior to conformational asymmetry, which produces a nonlocal excess entropy of mixing and has been predicted to increase the χ parameter over the value associated with enthalpic interactions.[70] How conformational asymmetry affects the composition dependence of χ is not well understood. As noted earlier, C and E are characterized by a large disparity in statistical segment length, which shifts the critical point to $\phi_{H,C}/\phi_H = 0.65$. Incorporation of both compositional and conformational asymmetry to the CE diblock copolymer may introduce compensating factors that result in the invariant homopolymer composition for the Scott line. Interestingly, the effects of compositional asymmetry appear to be qualitatively different in the ordered *versus* multiphase regions of the phase prism.

Microemulsions. Symmetric ternary polymer blends have been reported to form DIS BμEs along the volumetrically symmetric isopleth. A similar bicontinuous morphology exists in pure diblock copolymer melts due to fluctuation effects, which leads to structuring of the DIS state with large variations in composition and a morphology that contains zero mean curvature and negative Gauss curvature.[72−75] Addition of equal amounts of homopolymer results in a band of fluctuating bicontinuity above the line of congruency (or more correctly the narrow LAM−DIS 2-phase boundary) up to approximately the Lifshitz composition $\phi_{H,LP}$. Numerous previous studies have identified a BμE channel between the LAM and multiphase region in the vicinity of $\phi_{H,LP}$ that extends down in temperatures to varying degrees.[4−15] The existence of this BμE channel has been attributed to fluctuation effects, which are predicted to destroy the LP and associated 3-phase region (A + B + LAM) predicted by mean-field theory ($N_{AB} \rightarrow \infty$, where N_{AB} is the diblock copolymer degree of polymerization)[31] as shown in Figure 11. However, recent field

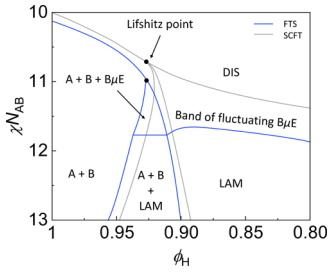

Figure 11. Sketches of phase diagrams along the volumetrically symmetric isopleth calculated by FTS and SCFT for a conformationally and compositionally symmetric A/B/AB ternary blend system.[56] Adapted with permission from ref 56.

theoretic simulations (FTS) by Vorselaars *et al.* on compositionally and conformationally symmetric ternary mixtures ($\bar{N}_{AB} = 5 \times 10^4$, where $\bar{N}_{AB}$ is the invariant degree of polymerization) show that subtle differences in free energy favor a three-phase window between the LAM and 2-phase (A + B) regions at high χN_{AB} and a second three-phase window between BμE and two-phase (A + B) regions at lower χN_{AB}, terminating at a tricritical point (Figure 11).[56] Note that the FTS phase behavior reduces to the self-consistent field theory (SCFT) results when $N_{AB} \rightarrow \infty$. The three-phase coexistence (A + B + BμE) shrinks into the mean-field LP, and other phase boundaries shift continuously toward the mean-field locations.

Several factors conspire to distort the picture predicted theoretically for ideal ternary mixtures ($N_A = N_B = 0.2N_{AB}$ and $f_A = 0.5$ with $b_A = b_B$) and generally presumed to apply to actual experimental systems. An example is conformational asymmetry, which has been shown recently to shift the location of the congruent LAM−DIS transition along with the critical composition of the homopolymer blend away from the symmetric isopleth ($\phi_{H,C}/\phi_H = 0.5$).[12] A narrow channel in composition ($\Delta\phi_H < 0.01$) located where the extrapolated congruent and Scott lines meet was associated with BμE. The work presented here illustrates how diblock copolymer compositional asymmetry shifts the LAM−DIS line of congruent transitions from $\phi_{H,C}/\phi_H = 0.6$ to $\phi_{H,C}/\phi_H = 0.42$, while leaving the location of the Scott line virtually unaffected. This opens up a wide range of disorder toward the middle of the phase prism (see Figure 4), which contains structured microemulsions as evidenced by the SANS patterns shown in Figures 9 and 10. Microemulsions along the congruent isopleth are expected to be bicontinuous, although the actual extent of co-continuity likely depends on the volume fractions of C and E. Similar to the transition from BμEs to droplet microemulsions in water/oil/surfactant mixtures upon varying the composition and temperature, we anticipate that increasing or decreasing the amount of E or C away from the condition of zero mean curvature reduces the extent of domain connectivity. While the SANS patterns obtained near the multiphase region in the phase prism at $\phi_H \geq 0.8$ and $\phi_{H,C}/\phi_H = 0.65$ are quantitatively accounted for by the T−S model (Figure 10), we cannot assign an average interfacial mean curvature or extent of bicontinuity solely based on these fits. A preferred interfacial curvature toward either C or E domains could drive the system to adopt a tubular or even droplet microemulsion morphology. Establishing the actual microemulsion structure requires either real-space imaging such as transmission electron microscopy (TEM) or a property measurement sensitive to this feature, such as conductivity. Unfortunately, microemulsion samples prepared along the Scott line composition were too brittle to allow microtoming of thin sections for application of TEM, and these polymers are insulators, thus obviating the use of conductivity measurements.

In general, the interfacial curvature and thus the domain connectivity can be adjusted by tuning the ratio of homopolymer volume fractions. The congruent transition can be determined in order to locate the conditions most conducive to the formation of BμEs. This is, in fact, one of the key advantages of studying ternary polymer blends, as any asymmetry in block copolymers and/or homopolymers, such as the conformational and compositional asymmetries discussed in this report, and other asymmetries such as the difference in dispersity of each block,[8,76,77] can be compensated by tuning the homopolymer content. Overall, the results found in this study have important implications for the design of ternary polymer blends to prepare co-continuous functional materials.

CONCLUSIONS

In this study, we describe the phase behavior of C/E/CE ternary polymer blends with a compositionally asymmetric diblock copolymer ($f_C = 0.67$) and symmetric homopolymers ($N_C \cong N_E$). The phase behavior, including blend morphologies and phase boundaries, was established using a combination of optical transmission, SAXS, and SANS measurements.

https://dx.doi.org/10.1021/acs.macromol.0c01745
Macromolecules 2021, 54, 460−472

Introduction of the diblock copolymer compositional asymmetry shifts the locations of the ordered phases in the phase prism, defined by the three composition variables ($\phi_{H,C}$, $\phi_{H,E}$, and ϕ_{CE}) and temperature, relative to previous results obtained with $f_C = 0.5$.[12] A key finding is that the composition of the (nearly) congruent LAM−DIS transitions near the multiphase region at a high homopolymer content shifts from $\phi_{H,C}/\phi_H = 0.6$ when $f_C = 0.5$ to $\phi_{H,C}/\phi_H = 0.42$ when $f_C = 0.67$. However, the change in the diblock copolymer symmetry does not affect the composition of the Scott line of critical points, which remains coupled to the binary homopolymer critical composition $\phi_{H,C}/\phi_H = 0.65$. Thus, the congruent and Scott lines are decoupled in composition by the introduction of compositional asymmetry of the diblock copolymer. Interestingly, a wide range of phase space between the compositions associated with the congruent and Scott lines is shown to contain a microemulsion morphology.

■ ASSOCIATED CONTENT

Supporting Information

The Supporting Information is available free of charge at https://pubs.acs.org/doi/10.1021/acs.macromol.0c01745.

SEC traces; cylinder form factor; optical transmission results; cloud point data; SANS profiles; and Scott line calculation (PDF)

■ AUTHOR INFORMATION

Corresponding Authors

Timothy P. Lodge − *Department of Chemical Engineering and Materials Science and Department of Chemistry, University of Minnesota, Minneapolis, Minnesota 55455, United States;* orcid.org/0000-0001-5916-8834; Email: lodge@umn.edu

Frank S. Bates − *Department of Chemical Engineering and Materials Science, University of Minnesota, Minneapolis, Minnesota 55455, United States;* orcid.org/0000-0003-3977-1278; Email: bates001@umn.edu

Authors

Bo Zhang − *Department of Chemical Engineering and Materials Science, University of Minnesota, Minneapolis, Minnesota 55455, United States;* orcid.org/0000-0001-5366-1855

Shuyi Xie − *Department of Chemistry, University of Minnesota, Minneapolis, Minnesota 55455, United States;* orcid.org/0000-0001-7966-1239

Complete contact information is available at: https://pubs.acs.org/10.1021/acs.macromol.0c01745

Notes

The authors declare no competing financial interest.

■ ACKNOWLEDGMENTS

This work was supported by the Office of Basic Energy Sciences (BES) of the U.S. Department of Energy (DoE), under contract no. DE-FOA-0001664. We acknowledge the support of the National Institute of Standard and Technology, U.S. Department of Commerce, in providing the neutron research facilities used in this work, and thank our local contact Yimin Mao for setting up the SANS instruments. Portions of this work were performed at the DuPont-Northwestern-Dow Collaborative Access Team (DND-CAT) located at Sector 5 of the Advanced Photon Source (APS). DND-CAT is supported by Northwestern University, The Dow Chemical Company, and DuPont de Nemours, Inc. This research used resources of the Advanced Photon Source, a U.S. Department of Energy (DoE) Office of Science User Facility operated for the DoE Office of Science by the Argonne National Laboratory under contract no. DE-AC02-06CH11357. Parts of this work were carried out in the Characterization Facility at the University of Minnesota, which receives partial support from the NSF through the MRSEC program (DMR-2011401).

■ REFERENCES

(1) Kahlweit, M.; Strey, R. Phase behavior of ternary systems of the type H_2O-oil-nonionic amphiphile (microemulsions). *Angew. Chem., Int. Ed.* **1985**, *24*, 654−668.

(2) Olsson, U.; Shinoda, K.; Lindman, B. Change of the structure of microemulsions with the hydrophile-lipophile balance of nonionic surfactant as revealed by NMR self-diffusion studies. *J. Phys. Chem.* **1986**, *90*, 4083−4088.

(3) Kahlweit, M. Microemulsions. *Science* **1988**, *240*, 617−621.

(4) Bates, F. S.; Maurer, W. W.; Lipic, P. M.; Hillmyer, M. A.; Almdal, K.; Mortensen, K.; Fredrickson, G. H.; Lodge, T. P. Polymeric bicontinuous microemulsions. *Phys. Rev. Lett.* **1997**, *79*, 849−852.

(5) Hillmyer, M. A.; Maurer, W. W.; Lodge, T. P.; Bates, F. S.; Almdal, K. Model bicontinuous microemulsions in ternary homopolymer block copolymer blends. *J. Phys. Chem. B* **1999**, *103*, 4814−4824.

(6) Washburn, N. R.; Lodge, T. P.; Bates, F. S. Ternary polymer blends as model surfactant systems. *J. Phys. Chem. B* **2000**, *104*, 6987−6997.

(7) Zhou, N.; Lodge, T. P.; Bates, F. S. Influence of conformational asymmetry on the phase behavior of ternary homopolymer/block copolymer blends around the bicontinuous microemulsion channel. *J. Phys. Chem. B* **2006**, *110*, 3979−3989.

(8) Ellison, C. J.; Meuler, A. J.; Qin, J.; Evans, C. M.; Wolf, L. M.; Bates, F. S. Bicontinuous polymeric microemulsions from polydisperse diblock copolymers. *J. Phys. Chem. B* **2009**, *113*, 3726−3737.

(9) Habersberger, B. M.; Bates, F. S.; Lodge, T. P. Hierarchical microphase separation in bicontinuous ternary polymer blends. *Soft Matter* **2012**, *8*, 3429−3441.

(10) Habersberger, B. M.; Gillard, T. M.; Hickey, R. J.; Lodge, T. P.; Bates, F. S. Fluctuation effects in symmetric diblock copolymer-homopolymer ternary mixtures near the lamellar-disorder transition. *ACS Macro Lett.* **2014**, *3*, 1041−1045.

(11) Hickey, R. J.; Gillard, T. M.; Irwin, M. T.; Lodge, T. P.; Bates, F. S. Structure, viscoelasticity, and interfacial dynamics of a model polymeric bicontinuous microemulsion. *Soft Matter* **2016**, *12*, 53−66.

(12) Hickey, R. J.; Gillard, T. M.; Irwin, M. T.; Morse, D. C.; Lodge, T. P.; Bates, F. S. Phase behavior of diblock copolymer-homopolymer ternary blends: Congruent first-order lamellar-disorder transition. *Macromolecules* **2016**, *49*, 7928−7944.

(13) Corvazier, L.; Messé, L.; Salou, C. L. O.; Young, R. N.; Fairclough, J. P. A.; Ryan, A. J. Lamellar phases and microemulsions in model ternary blends containing amphiphilic block copolymers. *J. Mater. Chem.* **2001**, *11*, 2864−2874.

(14) Messé, L.; Corvazier, L.; Ryan, A. J. Effect of the molecular weight of the homopolymers on the morphology in ternary blends of polystyrene, polyisoprene, polystyrene-block-polyisoprene copolymer. *Polymer* **2003**, *44*, 7397−7403.

(15) Jeon, H. S.; Lee, J. H.; Balsara, N. P.; Newstein, M. C. An experimental study of the thermodynamic properties of multicomponent polyolefin blends with ordered and disordered phases. *Macromolecules* **1998**, *31*, 3340−3352.

(16) Lee, J. H.; Ruegg, M. L.; Balsara, N. P.; Zhu, Y.; Gido, S. P.; Krishnamoorti, R.; Kim, M.-H. Phase behavior of highly immiscible polymer blends stabilized by a balanced block copolymer surfactant. *Macromolecules* **2003**, *36*, 6537−6548.

(17) Reynolds, B. J.; Ruegg, M. L.; Balsara, N. P.; Radke, C. J.; Shaffer, T. D.; Lin, M. Y.; Shull, K. R.; Lohse, D. J. Thermodynamics of polymer blends organized by balanced block copolymer surfactants studied by mean-field theories and scattering. *Macromolecules* **2004**, *37*, 7401−7417.
(18) Ruegg, M. L.; Reynolds, B. J.; Lin, M. Y.; Lohse, D. J.; Balsara, N. P. Minimizing the concentration of diblock copolymer needed to organize blends of weakly segregated polymers by tuning attractive and repulsive interactions. *Macromolecules* **2007**, *40*, 1207−1217.
(19) Zhou, N.; Bates, F. S.; Lodge, T. P. Mesoporous membrane templated by a polymeric bicontinuous microemulsion. *Nano Lett.* **2006**, *6*, 2354−2357.
(20) Jones, B. H.; Lodge, T. P. High-temperature nanoporous ceramic monolith prepared from a polymeric bicontinuous microemulsion template. *J. Am. Chem. Soc.* **2009**, *131*, 1676−1677.
(21) Jones, B. H.; Lodge, T. P. Nanoporous materials derived from polymeric bicontinuous microemulsions. *Chem. Mater.* **2010**, *22*, 1279−1281.
(22) Jones, B. H.; Lodge, T. P. Hierarchically structured materials from block polymer confinement within bicontinuous microemulsion-derived nanoporous polyethylene. *ACS Nano* **2011**, *5*, 8914−8927.
(23) Jones, B. H.; Cheng, K.-Y.; Holmes, R. J.; Lodge, T. P. Nanoporous poly(3,4-ethylenedioxythiophene) derived from polymeric bicontinuous microemulsion templates. *Macromolecules* **2012**, *45*, 599−601.
(24) Jones, B. H.; Lodge, T. P. Nanocasting nanoporous inorganic and organic materials from polymeric bicontinuous microemulsion templates. *Polym. J.* **2012**, *44*, 131−146.
(25) Kipp, D.; Wodo, O.; Ganapathysubramanian, B.; Ganesan, V. Achieving bicontinuous microemulsion like morphologies in organic photovoltaics. *ACS Macro Lett.* **2015**, *4*, 266−270.
(26) Bates, F. S.; Fredrickson, G. H. Block copolymer thermodynamics: Theory and experiment. *Annu. Rev. Phys. Chem.* **1990**, *41*, 525−557.
(27) Bates, F. S. Polymer-polymer phase behavior. *Science* **1991**, *251*, 898−905.
(28) Bates, F. S.; Fredrickson, G. H. Block Copolymers-Designer Soft Materials. *Phys. Today* **1999**, *52*, 32−38.
(29) Leibler, L. Theory of microphase separation in block copolymers. *Macromolecules* **1980**, *13*, 1602−1617.
(30) Broseta, D.; Fredrickson, G. H. Phase equilibria in copolymer/homopolymer ternary blends: Molecular weight effects. *J. Chem. Phys.* **1990**, *93*, 2927−2938.
(31) Düchs, D.; Ganesan, V.; Fredrickson, G. H.; Schmid, F. Fluctuation effects in ternary AB + A + B polymeric emulsions. *Macromolecules* **2003**, *36*, 9237−9248.
(32) Bates, F. S. Block copolymers near the microphase separation transition. 2. Linear dynamic mechanical properties. *Macromolecules* **1984**, *17*, 2607−2613.
(33) Bates, F. S.; Rosedale, J. H.; Fredrickson, G. H.; Glinka, C. J. Fluctuation-induced first-order transition of an isotropic system to a periodic state. *Phys. Rev. Lett.* **1988**, *61*, 2229−2232.
(34) Fredrickson, G. H.; Helfand, E. Fluctuation effects in the theory of microphase separation in block copolymers. *J. Chem. Phys.* **1987**, *87*, 697−705.
(35) Bates, F. S.; Rosedale, J. H.; Fredrickson, G. H. Fluctuation effects in a symmetric diblock copolymer near the order-disorder transition. *J. Chem. Phys.* **1990**, *92*, 6255−6270.
(36) Rosedale, J. H.; Bates, F. S. Rheology of ordered and disordered symmetric poly(ethyleneпropylene)-poly(ethylethylene) diblock copolymers. *Macromolecules* **1990**, *23*, 2329−2338.
(37) Rosedale, J. H.; Bates, F. S.; Almdal, K.; Mortensen, K.; Wignall, G. D. Order and disorder in symmetric diblock copolymer melts. *Macromolecules* **1995**, *28*, 1429−1443.
(38) Brazovskii, S. A. Phase transition of an isotropic system to a nonuniform state. *J. Exp. Theor. Phys.* **1975**, *41*, 85−89.
(39) Herkt-Maetzky, C.; Schelten, J. Critical fluctuations in a binary polymer mixture. *Phys. Rev. Lett.* **1983**, *51*, 896−899.
(40) Schwahn, D.; Mortensen, K.; Yee-Madeira, H. Mean-field and Ising critical behavior of a polymer blend. *Phys. Rev. Lett.* **1987**, *58*, 1544−1546.
(41) Bates, F.; Rosedale, J.; Stepanek, P.; Lodge, T.; Wiltzius, P.; Fredrickson, G.; Hjelm, R., Jr. Static and dynamic crossover in a critical polymer mixture. *Phys. Rev. Lett.* **1990**, *65*, 1893−1896.
(42) Janssen, S.; Schwahn, D.; Springer, T. Mean-field Ising crossover and the critical exponents γ, ν, and η for a polymer blend:d-PB/PS studied by small-angle neutron scattering. *Phys. Rev. Lett.* **1992**, *68*, 3180−3183.
(43) Bates, F. S.; Maurer, W.; Lodge, T. P.; Schulz, M. F.; Matsen, M. W.; Almdal, K.; Mortensen, K. Isotropic Lifshitz behavior in block copolymer-homopolymer blends. *Phys. Rev. Lett.* **1995**, *75*, 4429−4432.
(44) Schwahn, D.; Mortensen, K.; Frielinghaus, H.; Almdal, K. Crossover from 3D Ising to isotropic Lifshitz critical behavior in a mixture of a homopolymer blend and diblock copolymer. *Phys. Rev. Lett.* **1999**, *82*, 5056−5059.
(45) Schwahn, D.; Mortensen, K.; Frielinghaus, H.; Almdal, K.; Kielhorn, L. Thermal composition fluctuations near the isotropic Lifshitz critical point in a ternary mixture of a homopolymer blend and diblock copolymer. *J. Chem. Phys.* **2000**, *112*, 5454−5472.
(46) Pipich, V.; Schwahn, D.; Willner, L. Ginzburg number of a homopolymer-diblock copolymer mixture covering the 3D-Ising, isotropic Lifshitz, and Brasovskii classes of critical universality. *Phys. Rev. Lett.* **2005**, *94*, 117801.
(47) Pipich, V.; Schwahn, D.; Willner, L. Composition fluctuations in a homopolymer-diblock copolymer mixture covering the three-dimensional Ising, isotropic Lifshitz, and Brasovskiĭ classes of critical universality. *J. Chem. Phys.* **2005**, *123*, 124904.
(48) Pipich, V.; Willner, L.; Schwahn, D. The A-B diblock copolymer as a nonordering external field in a three-component A/B/A-B polymer blend. *J. Phys. Chem. B* **2008**, *112*, 16170−16181.
(49) Irwin, M. T.; Hickey, R. J.; Xie, S.; Bates, F. S.; Lodge, T. P. Lithium salt-induced microstructure and ordering in diblock copolymer/homopolymer blends. *Macromolecules* **2016**, *49*, 4839−4849.
(50) Irwin, M. T.; Hickey, R. J.; Xie, S.; So, S.; Bates, F. S.; Lodge, T. P. Structure-conductivity relationships in ordered and disordered salt-doped diblock copolymer/homopolymer blends. *Macromolecules* **2016**, *49*, 6928−6939.
(51) Xie, S.; Meyer, D. J.; Wang, E.; Bates, F. S.; Lodge, T. P. Structure and properties of bicontinuous microemulsions from salt-doped ternary polymer blends. *Macromolecules* **2019**, *52*, 9693−9702.
(52) Shim, J.; Bates, F. S.; Lodge, T. P. Bicontinuous microemulsions in partially charged ternary polymer blends. *ACS Macro Lett.* **2019**, *8*, 1166−1171.
(53) Shim, J.; Xie, S.; Bates, F. S.; Lodge, T. P. Effect of ion concentration on the formation of bicontinuous microemulsions in partially charged ternary polymer blends. *Macromolecules* **2019**, *52*, 9416−9424.
(54) Kielhorn, L.; Muthukumar, M. Fluctuation theory of diblock copolymer/homopolymer blends and its effects on the Lifshitz point. *J. Chem. Phys.* **1997**, *107*, 5588−5608.
(55) Spencer, R. K. W.; Matsen, M. W. Fluctuation effects in blends of A + B homopolymers with AB diblock copolymer. *J. Chem. Phys.* **2018**, *148*, 204907.
(56) Vorselaars, B.; Spencer, R. K. W.; Matsen, M. W. Instability of the microemulsion channel in block copolymer-homopolymer blends. *Phys. Rev. Lett.* **2020**, *125*, 117801.
(57) Cochran, E. W.; Bates, F. S. Thermodynamic behavior of poly(cyclohexylethylene) in polyolefin diblock copolymers. *Macromolecules* **2002**, *35*, 7368−7374.
(58) Fetters, L. J.; Lohse, D. J.; Richter, D.; Witten, T. A.; Zirkel, A. Connection between polymer molecular-weight, density, chain dimensions, and melt viscoelastic properties. *Macromolecules* **1994**, *27*, 4639−4647.

https://dx.doi.org/10.1021/acs.macromol.0c01745
Macromolecules 2021, 54, 460−472

(59) Balsara, N. P.; Perahia, D.; Safinya, C. R.; Tirrell, M.; Lodge, T. P. Birefringence detection of the order-to-disorder transition in block copolymer liquids. *Macromolecules* **1992**, *25*, 3896−3901.
(60) Flory, P. J. Thermodynamics of high polymer solutions. *J. Chem. Phys.* **1942**, *10*, 51−61.
(61) Huggins, M. L. Theory of solutions of high polymers. *J. Am. Chem. Soc.* **1942**, *64*, 1712−1719.
(62) de Gennes, P.-G. *Scaling Concepts in Polymer Physics*; Cornell University Press: Ithaca, N.Y., 1979.
(63) Teubner, M.; Strey, R. Origin of the scattering peak in microemulsions. *J. Chem. Phys.* **1987**, *87*, 3195−3200.
(64) Schubert, K. V.; Strey, R.; Kline, S. R.; Kaler, E. W. Small angle neutron scattering near Lifshitz lines: Transition from weakly structured mixtures to microemulsions. *J. Chem. Phys.* **1994**, *101*, 5343−5355.
(65) Bates, F. S.; Wiltzius, P. Spinodal decomposition of a symmetric critical mixture of deuterated and protonated polymer. *J. Chem. Phys.* **1989**, *91*, 3258−3274.
(66) Matsen, M. W.; Bates, F. S. Conformationally asymmetric block copolymers. *J. Polym. Sci., Part B: Polym. Phys.* **1997**, *35*, 945−952.
(67) Khandpur, A. K.; Foerster, S.; Bates, F. S.; Hamley, I. W.; Ryan, A. J.; Bras, W.; Almdal, K.; Mortensen, K. Polyisoprene-polystyrene diblock copolymer phase diagram near the order-disorder transition. *Macromolecules* **1995**, *28*, 8796−8806.
(68) Matsen, M. W.; Schick, M. Microphases of a diblock copolymer with conformational asymmetry. *Macromolecules* **1994**, *27*, 4014−4015.
(69) Vavasour, J. D.; Whitmore, M. D. Self-consistent field theory of block copolymers with conformational asymmetry. *Macromolecules* **1993**, *26*, 7070−7075.
(70) Bates, F. S.; Fredrickson, G. H. Conformational asymmetry and polymer-polymer thermodynamics. *Macromolecules* **1994**, *27*, 1065−1067.
(71) Yadav, M.; Bates, F. S.; Morse, D. C. Effects of segment length asymmetry in ternary diblock copolymer−homopolymer mixtures. *Macromolecules* **2019**, *52*, 4091−4102.
(72) Hampu, N.; Bates, M. W.; Vidil, T.; Hillmyer, M. A. Bicontinuous porous nanomaterials from block polymers radically cured in the disordered state for size-selective membrane applications. *ACS Appl. Nano Mater.* **2019**, *2*, 4567−4577.
(73) Hampu, N.; Hillmyer, M. A. Temporally controlled curing of block polymers in the disordered state using thermally stable photoacid generators for the preparation of nanoporous membranes. *ACS Appl. Polym. Mater.* **2019**, *1*, 1148−1154.
(74) Hampu, N.; Hillmyer, M. A. Molecular engineering of nanostructures in disordered block polymers. *ACS Macro Lett.* **2020**, *9*, 382−388.
(75) Lee, S.; Gillard, T. M.; Bates, F. S. Fluctuations, order, and disorder in short diblock copolymers. *AIChE J.* **2013**, *59*, 3502−3513.
(76) Lynd, N. A.; Hillmyer, M. A. Influence of polydispersity on the self-assembly of diblock copolymers. *Macromolecules* **2005**, *38*, 8803−8810.
(77) Lynd, N. A.; Meuler, A. J.; Hillmyer, M. A. Polydispersity and block copolymer self-assembly. *Prog. Polym. Sci.* **2008**, *33*, 875−893.

https://dx.doi.org/10.1021/acs.macromol.0c01745
Macromolecules 2021, 54, 460−472